MOLECULAR AND CELLULAR BIOLOGY, Aug. 2006, p. 5621–5635 Vol. 26, No. 15
0270-7306/06/$08.00+0 doi:10.1128/MCB.02357-05

The Normal Phenotype of Pmm1-Deficient Mice Suggests that Pmm1 Is Not Essential for Normal Mouse Development

K. Cromphout,[1] W. Vleugels,[1] L. Heykants,[1] E. Schollen,[1] L. Keldermans,[1] R. Sciot,[2] R. D'Hooge,[3] P. P. De Deyn,[4] K. von Figura,[5] D. Hartmann,[6] C. Körner,[7] and G. Matthijs[1]*

Center for Human Genetics, Katholieke Universiteit Leuven, Leuven, Belgium[1]; Department of Pathology, Katholieke Universiteit Leuven, Leuven, Belgium[2]; Laboratory of Biological Psychology, Department of Psychology, Katholieke Universiteit Leuven, Leuven, Belgium[3]; Laboratory of Neurochemistry and Behavior, Born-Bunge Institute, University of Antwerp, Antwerp, Belgium[4]; Biochemistry II, University of Goettingen, Goettingen, Germany[5]; Center for Human Genetics and Flanders Interuniversity Institute for Biotechnology, VIB4, Katholieke Universiteit Leuven, Leuven, Belgium[6]; and Universitätskinderklinik, Uni-Heidelberg, Heidelberg, Germany[7]

Received 10 December 2005/Returned for modification 26 February 2006/Accepted 25 April 2006

Phosphomannomutases (PMMs) are crucial for the glycosylation of glycoproteins. In humans, two highly conserved PMMs exist: PMM1 and PMM2. In vitro both enzymes are able to convert mannose-6-phosphate (mannose-6-P) into mannose-1-P, the key starting compound for glycan biosynthesis. However, only mutations causing a deficiency in PMM2 cause hypoglycosylation, leading to the most frequent type of the congenital disorders of glycosylation (CDG): CDG-Ia. PMM1 is as yet not associated with any disease, and its physiological role has remained unclear. We generated a mouse deficient in Pmm1 activity and documented the expression pattern of murine Pmm1 to unravel its biological role. The expression pattern suggested an involvement of Pmm1 in (neural) development and endocrine regulation. Surprisingly, Pmm1 knockout mice were viable, developed normally, and did not reveal any obvious phenotypic alteration up to adulthood. The macroscopic and microscopic anatomy of all major organs, as well as animal behavior, appeared to be normal. Likewise, lectin histochemistry did not demonstrate an altered glycosylation pattern in tissues. It is especially striking that Pmm1, despite an almost complete overlap of its expression with Pmm2, e.g., in the developing brain, is apparently unable to compensate for deficient Pmm2 activity in CDG-Ia patients. Together, these data point to a (developmental) function independent of mannose-1-P synthesis, whereby the normal knockout phenotype, despite the stringent conservation in phylogeny, could be explained by a critical function under as-yet-unidentified challenge conditions.

N glycosylation of proteins is initiated with the synthesis of a stereotyped oligosaccharide precursor, $Glc_3Man_9GlcNAc_2$, in the endoplasmic reticulum. This precursor is then transferred to the nascent protein and further remodeled in the Golgi apparatus to end up as the complex carbohydrate structure found on mature glycoproteins. Correct N glycosylation requires a biochemical assembly line of closely interacting enzymes catalyzing the various steps in the pathway (1).

Phosphomannomutase 2 (PMM2) is a key enzyme in the initial steps of N glycosylation. PMM2 catalyzes the conversion of mannose-6-P to mannose-1-P (21), which, through the binding of GTP, generates GDP-mannose. This GDP-mannose is the source of the mannose core of the N-glycan precursors (1).

Mutations in the PMM2 gene result in reduced phosphomannomutase activity (18, 19, 23) and depletion of the GDP-mannose pool. As a result, numerous serum (e.g., transferrin, haptoglobin, and α_1-antitrypsin) (4, 26, 28) and cerebrospinal fluid glycoproteins (e.g., transferrin and β-trace protein) (9, 11, 24) in CDG-Ia patients are underglycosylated, whereas many lysosomal and other cellular enzymes loose their activity, probably also as a result of the hypoglycosylation (17). This hypoglycosylation causes a severe clinical syndrome characterized by developmental abnormalities of mainly the nervous system (featuring cerebellar hypoplasia and demyelinization) and peripheral neuropathy, resulting in a generalized psychomotor retardation. Severe cases present additional failure of single or multiple visceral organs. Most often the liver, heart, gut, and/or kidney are affected (16). The severe consequences of a reduced PMM2 activity are puzzling, since in humans another PMM gene, PMM1 was identified (20, 27). PMM1 displays 66% homology to PMM2 on an amino acid level and 65% on a nucleotide level. A comparison of the genomic structure of the PMMs indicated that the genes have probably arisen by gene duplication 75 to 110 million years ago (13, 25). The PMMs are highly conserved during evolution: the murine genes are located on syntenic regions and display 90% identity with the human genes. The presence of these two highly conserved PMM genes in the genome implies that both have crucial functions, whereby the physiologic role of PMM1 has remained elusive. Specifically, PMM1 is not implicated in any known disease (20–22), and solely mutations of PMM2 that cause a reduced enzyme activity (loss-of-function seems to be intolerable) are associated with disease, i.e., CDG-Ia. Since both the subcellular localization and the catalytic abilities are quite similar, it is counterintuitive that the PMM1 enzyme does not compensate for the reduced PMM2 activity and argues for a function unrelated to mannose-1-P synthesis.

In line with this reasoning, some biochemical differences between both PMMs have been identified. Besides its phos-

* Corresponding author. Mailing address: University of Leuven, Center for Human Genetics, Herestraat 49, 3000 Leuven, Belgium. Phone: 32 16 346070. Fax: 32 16 346060. E-mail: Gert.Matthijs@med.kuleuven.be.

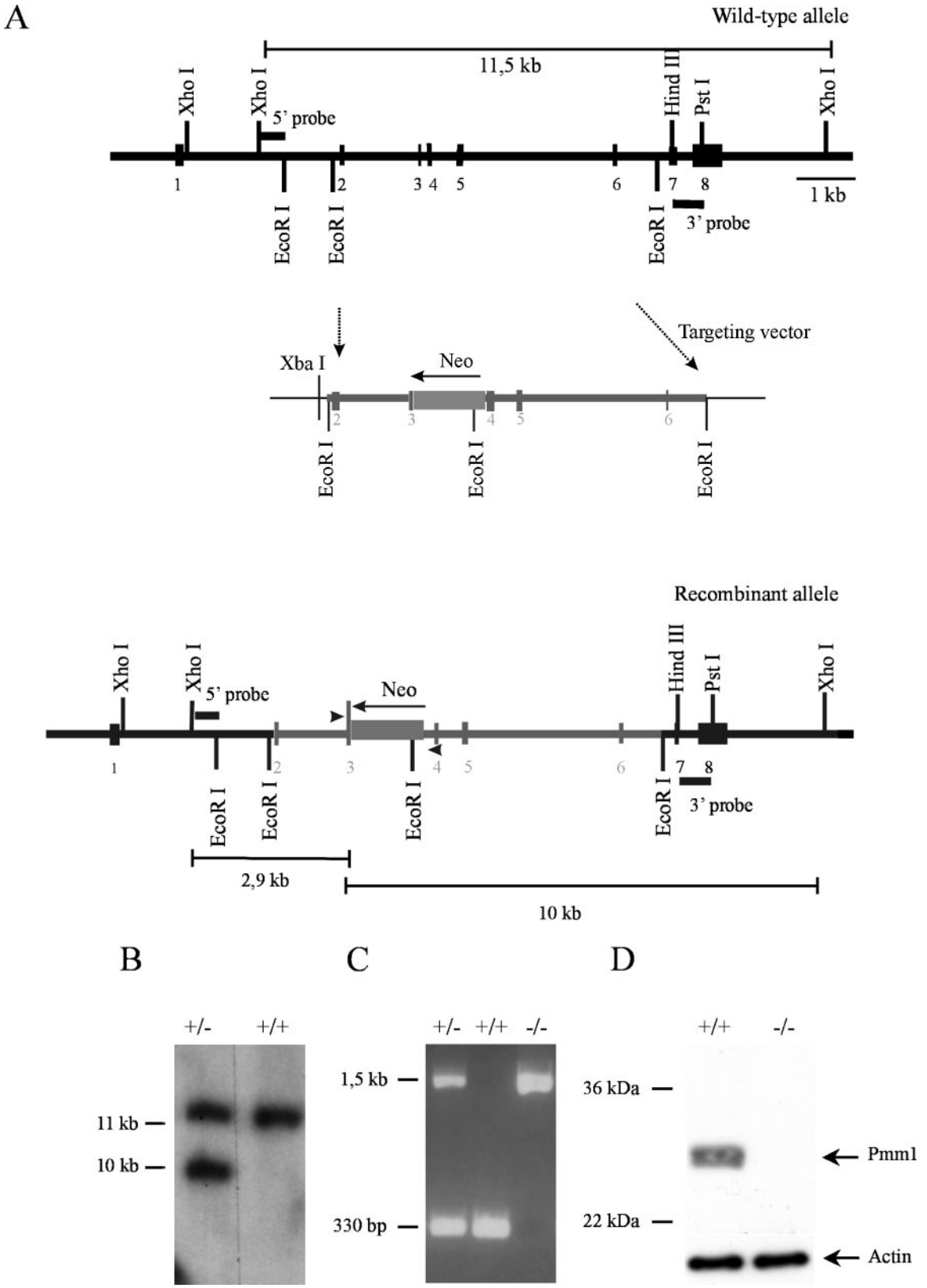

FIG. 1. Generation of Pmm1 knockout mice. (A) Generation of the targeting vector. A partial restriction map of the wild-type allele of Pmm1 is shown. To disrupt exon 3 in the mouse genome, a 6-kb EcoRI fragment, including exons 2 to 6 was subcloned into pBSK targeting vector. The Neo gene contains stop codons in all three reading frames. Homologous recombination between genomic DNA and the targeting vector results in the insertion of a 1.25-kb Neo cassette in exon 3. (B) Southern blot analysis of $Pmm1^{+/-}$ ES cells. Southern blot analysis was carried out on XhoI-digested genomic DNA from G418-resistant ES clones with the 3′ external probe, a HindIII/PstI fragment 3′ of the homologous region (see

phomannomutase activity in vitro, PMM1 has an additional phosphoglucomutase activity and in vitro also converts glucose-1-P into glucose-6-P, whereas PMM2 converts glucose-1-P 20 times more slowly than mannose-1-P. PMM1 has a higher K_a value for both mannose-1,6-bisphosphate and glucose-1,6-bisphosphate compared to the K_a values for PMM2. Fructose-1,6-bisphosphate can also stimulate PMM1, in contrast to PMM2. When incubated with fructose-1,6-bisphosphate, PMM2 activity depends on the formation of mannose-1,6-bisphosphate from fructose-1,6-bisphosphate and mannose-1-phosphate by PMM1 (21).

The phosphomannomutases not only differ in kinetics. Previous Northern blot analysis on adult human tissues has indicated some differences in expression pattern. PMM1 mRNA was abundant in brain, liver, pancreas, kidney, skeletal muscle, and heart samples, and lower levels were detected in placenta and lungs. Highest expression of PMM2 was found in pancreas, liver, kidney, and placenta. Skeletal muscle, heart, and lung showed lower PMM2 levels, whereas in brain almost no signal was observed (19, 20). These results suggest PMM1 is the brain specific phosphomannomutase, which is in contrast with the patient's clinical picture of severe neurological involvement due to decreased PMM2 activity.

To unravel the biological role of PMM1 and PMM2, the murine orthologous genes were previously cloned (13), and their expression in adult mice was analyzed on a Northern blot. In comparison to the published human expression profile described above, this revealed a quite similar expression pattern for the murine Pmm1 and Pmm2 and especially showed high Pmm1 levels in adult mouse brain and visceral organs (13). Enzyme activity measurements of adult rat brain extracts after Pmm2 immunoprecipitation indicated that Pmm1 accounts for 66% of the total phosphomannomutase activity in brain (21).

To elucidate the physiological role of Pmm1 and to gain a better understanding of its expression profile within the tissues, we documented the expression pattern of the Pmm1 protein in embryonic and adult tissues of wild-type mice on the tissue level by immunohistochemistry and ISH. We especially expected additional insights into possible differences in the microdistribution of both enzymes that could have escaped Northern blot approaches. We then generated Pmm1-deficient mice and looked for phenotypic changes in adult mice and embryos. Glycan structures were studied by lectin glycohistochemical analysis of Pmm1-deficient tissues.

MATERIALS AND METHODS

Generation of Pmm1 knockout mice. All animal experiments were approved by the Institutional Ethical Committee of the Katholieke Universiteit Leuven, Belgium. All efforts were made to use the minimum number of animals necessary to obtain adequate scientific data.

For construction of the targeting vector, a pBSK vector (Stratagene) without XhoI restriction site was constructed by digestion with XhoI and HindIII and subsequent Klenow polymerase blunting of the overhangs and ligation. A 6-kb EcoRI subclone from the BACclone 85J13 (Research Genetics), containing the entire Pmm1 gene was inserted in this vector. This subclone consisted of a fragment containing the region between the last 50 bases of intron 1 and the first 750 bases of intron 6. Exon 3 of Pmm1 was mutated to create unique XhoI and NheI sites by insertion of a C and mutating a CT into GC, respectively. A XhoI-XbaI digestion thus resulted in a loss of 29 bp from exon 3 and allowed the insertion of a XhoI-XbaI PGK-Neo cassette in inverse orientation (Fig. 1A).

The resulting plasmid had homologous regions of at least 1.5 kb flanking the Neo-cassette and contained a unique restriction site in the vector for XbaI. After transfection of E14-1 embryonic stem (ES) cells with the linearized targeting vector, selection was done with G418 during 10 days. A total of 176 ES cell clones were picked and frozen. Eighty clones were analyzed for homologous recombination by Southern hybridization of XhoI restricted DNA. For detection, two external probes (a XhoI-EcoRI fragment of 0.4 kb corresponding to the intron 1 sequence and a HindIII-PstI fragment of 0.8 kb corresponding to the region containing exon 7 and 8) outside the Neo cassette and one internal probe corresponding to the 1.25-kb Neo cassette were used. All clones were initially tested with the 5′ external probe. This probe would detect an 11.5-kb fragment on the wild-type allele and a 2.9-kb fragment on the knockout allele. This hybridization resulted in one positive clone (data not shown) that was further subjected to hybridization with the 3′ external probe. The clone had the expected mutant 10-kb XhoI fragment, whereas the fragment of the wild-type allele was 11.5 kb (Fig. 1B). ES cells from this clone were injected in blastocysts from C57BL/6J mice, and embryos were transferred to pseudopregnant females. A total of 19 pups were born, 8 of which were chimeric. Three chimeric males were bred with 21 C57BL/6J females to check for germ line transmission. DNA extracted from the tails of the F_1 generation was analyzed by PCR with the following primers located around the insertion site of the Neo cassette: AGGC AGAAGTTGATCAAGTC as the forward primer (in intron 2) and CGGTTT AGAGCGGAACAGA as the reverse primer (in exon 4). PCR resulted in fragments of 1.5 kb for the mutant and 330 bp for the wild-type fragment (Fig. 1C). All males were able to transmit the mutant allele and heterozygote males and females were intercrossed to generate homozygous mice. Homozygous mice did not express the Pmm1 enzyme or any truncated form of the protein as assayed by Western blotting of brain homogenates (Fig. 1D). Pmm1 knockout mice have a total phosphomannomutase activity of only 33% compared to wild-type mice. Because there is no assay to enzymatically distinguish between Pmm1 and Pmm2 (21), a simple immunoprecipitation experiment was performed on brain extracts from wild-type and mutant mice. Using a Pmm2 antibody, it was shown that the residual activity is below 3% in knockout mice and 70% in wild-type mice.

Behavioral assessment in Pmm1 knockout mice. Analysis for a behavioral phenotype was done by subjecting wild-type and knockout mice (aged 1 year) to a modified and extended version of the behavioral test battery described previously (6). To assess a variety of different functions, the battery included tests for locomotion and exploratory activity (cage activity test, open-field activity, dark-light transition, and social exploration test), gait and neuromotor coordination (walking pattern and rotarod), muscle strength (wire suspension test), and learning or memory (passive avoidance and Morris water maze).

Briefly, cage activity was tested by counting the number of beam crossings in a standard home cage equipped with three infrared beams during dusk-phase (2-h) and overnight (16-h) observation periods. Open-field recording was performed to evaluate the general exploratory behavior when mice were placed for 10 min in an open-field arena equipped with a camera. In addition, exploratory behavior was tested in a dark-light transition box. The number of transitions between the two chambers was measured as the number of infrared beam interruptions. A first beam was placed close to the dark box, and a second beam was located some distance from the dark compartment. To assess social and/or sexual exploration in male mice, different ambulatory measures were recorded in an open-field arena containing a round cage with two wild-type female mice.

Gait ability and rotarod performance were recorded to examine neuromotor coordination and motor learning. During four consecutive trials on an

panel A). The wild-type allele results in a 11.5-kb band and the knockout allele results in a 10-kb band. (C) PCR genotyping of Pmm1 knockout mice. PCR was done on genomic tail DNA with two primers: one 3′ primer and 5′ primer (arrowheads in panel A). The wild-type allele results in a 330-bp band, and the knockout allele results in a 1.5-kb band. (D) Western blot analysis of brain extracts of Pmm1$^{+/+}$ and Pmm1$^{-/-}$ mice using the anti-Pmm1 antibody. Pmm1 knockout mice show no detectable Pmm1 and equal intensity of the actin signal as a loading control.

TABLE 1. Lectins used and sugar/glycan specificities

Group	Abbreviation	Sugar specificity	Glycan structure specificity
Mannose or glucose group			
Concanavalin A	CON A	α-Mannose and α-glucose (nonreducing)	Mannose-rich and hybrid N-glycans
Lentil lectin	LCA	α-Mannose and α-glucose	Hybrid and complex N-glycans with core fucosylation
Pea lectin	PSA	α-Mannose and α-glucose	Hybrid and complex N-glycans with core fucosylation
N-Acetylglucosamine group			
Griffonia lectin 2	GSL2	α- and β-GlcNAc (nonreducing)	Hybrid and complex N-glycans, type 2 and 3 mucin O-glycans
Datura lectin	DSA	β-GlcNAc oligomers	Polylactosamine on type 2 mucin O-glycans
Tomato lectin	LEL	β-GlcNAc oligomers	Polylactosamine on type 2 mucin O-glycans
Potato lectin	STL	β-GlcNAc oligomers	Type 2 mucin O-glycans with terminal polylactosamine
Wheat germ agglutinin	WGA	β-*N*-Acetylchitotriose, GlcNAc oligo- and monomers	Sialylated hybrid and complex N-glycans, type 2 and 3 mucin O-glycans
Succinylated WGA	Succ. WGA	β-*N*-Acetylchitotriose, GlcNAc oligo- and monomers	Nonsialylated hybrid and complex N-glycans, type 2 and 3 mucin O-glycans
Galactose/*N*-acetylgalactosamine group			
Dolichos lectin	DBA	α-GalNAc (nonreducing)	Type 5 and 7 mucin O-glycans
Peanut lectin	PNA	β-Galactose (nonreducing)	Asialo β-galactosylated N-glycans, type 1 and 2 mucin O-glycans
Jacalin	Jacalin	α- and β-galactose (nonreducing)	Type 1 and 2 mucin O-glycans
Griffonia lectin 1	GSL 1	α-galactose and α-GalNAc	α-Galactosylated N-glycans and type 5 and 8 mucin O-glycans
Soy bean lectin	SBA	α-Galactose and α-GalNAc	Type 5 and 7 mucin O-glycans
Ricinus lectin	RCA 1	β-Galactose and β-GalNAc (nonreducing)	Asialo β-galactosylated N-glycans, type 1 and 2 mucin O-glycans
Vicia lectin	VVL	β-GalNAc (nonreducing) and Tn antigen	β-GalNAc on O- and N-glycans
Erythrina lectin	ECL	α- and β-galactose and α- and β-GalNAc	*N*-Acetyllactosamine structures on N-glycans
Sophora lectin	SJA	α- and β-galactose and α- and β-GalNAc	GalNAc structures on N-glycans, type 1, 2, and 3 mucin O-glycans
Fucose group			
Ulex lectin	UEA-I	α-L-Fuc (nonreducing)	H-type 2 antigen sequence on N- and O-glycans
Complex specificity			
Phaseolus lectin E	PHA-E	Galβ(1,4)GlcNAcβ (1,2)Man	Bi/tri-antennary, bisected complex N-glycans
Phaseolus lectin L	PHA-L	Galβ(1,4)GlcNAcβ(1,2)[Galβ(1,4) GlcNAcβ(1,6)]Man	Tri/tetra-antennary, nonbisected complex N-glycans

accelerating rotarod (4 to 40 rpm, 5 min), time on the rod was recorded for up to 300 s.

To test for muscle strength, mice were to grasp a wire with their forepaws, and their ability to remain suspended for 120 s was measured.

In the training trial of the passive avoidance test, mice were placed in the light compartment of a step-through box, and the latency to enter the dark compartment was recorded. After entry in the dark compartment, a mild footshock was delivered through the metal grid floor (0.3 mA, 1 s). In the retention test (24 h after training), the mice were again placed in the illuminated box, and latency to re-enter the dark compartment was timed. Morris water maze training consisted of eight acquisition trial blocks (each comprising four daily swim trials), followed by a retention test during which the hidden escape platform was removed from the pool (probe trial), and the search path of the mice was video tracked for 100 s.

Analysis of the Pmm1 expression pattern by Western blot and immunohistochemistry. Euthanasia of the animals, isolation, and processing of the tissues or whole embryos for either Western analysis or immunohistochemistry were done as described in reference 7. Tissues investigated included brain, intestine, pancreas, liver, lung, testis, ovary, and adrenal gland. Western blots were done with a specific affinity-purified polyclonal rabbit anti-mouse Pmm1 antibody as described previously (7). Western analysis of embryonic and adult non neural tissues (15 μg) required antibody concentration of 1 in 500 and overnight exposure. Blots of adult endocrine glands such as testis, ovary, and adrenal gland were exposed for only 5 to 10 min. In all tissues a specific band corresponding to Pmm1 was detected, except for lung tissues, where a smaller protein showed nonspecific cross-reactivity with our antibody.

Immunohistochemistry was done with a polyclonal anti-Pmm1 antiserum whose specificity had been previously demonstrated in brain (7). However, this antiserum revealed a nonspecific reaction in embryonic heart and acrosomes of spermatozoa (not shown).

Experiments were repeated on tissues from four different wild-type and knockout mice at adult or embryonic stages and showed comparable results.

To identify the Pmm1 positive cells in pancreatic islets, double stainings were performed with either a commercial anti-mouse glucagon (Sigma) or a anti-swine insulin antibody (Dako).

(Glyco)histochemical analysis of Pmm1 knockout mice. Brains isolated from different developmental stages (postnatal day 0 [P0], P7, P20, and adult), adult testis and whole embryos (embryonic day 17 [E17]) from C57BL/6J wild-type mice, and Pmm1 knockouts were analyzed by lectin histochemistry to check for possible aberrant glycan structures. The tissues were prepared as described in reference 7. Deparaffinized sections were incubated for 1 h at room temperature with the lectins summarized in Table 1, together with their nominal specificities (Vector Laboratories). Brain sections were screened with antibodies to GFAP (antiglial fibrillary acid protein SMI-22 antibody, marker of astroglial cells; Steinberger Monoclonal, Inc.) and F4/80 (microglial/macrophage marker). Bis-benzimide was used as a nuclear counterstain. Sections were covered in Vectashield (Vector Laboratories).

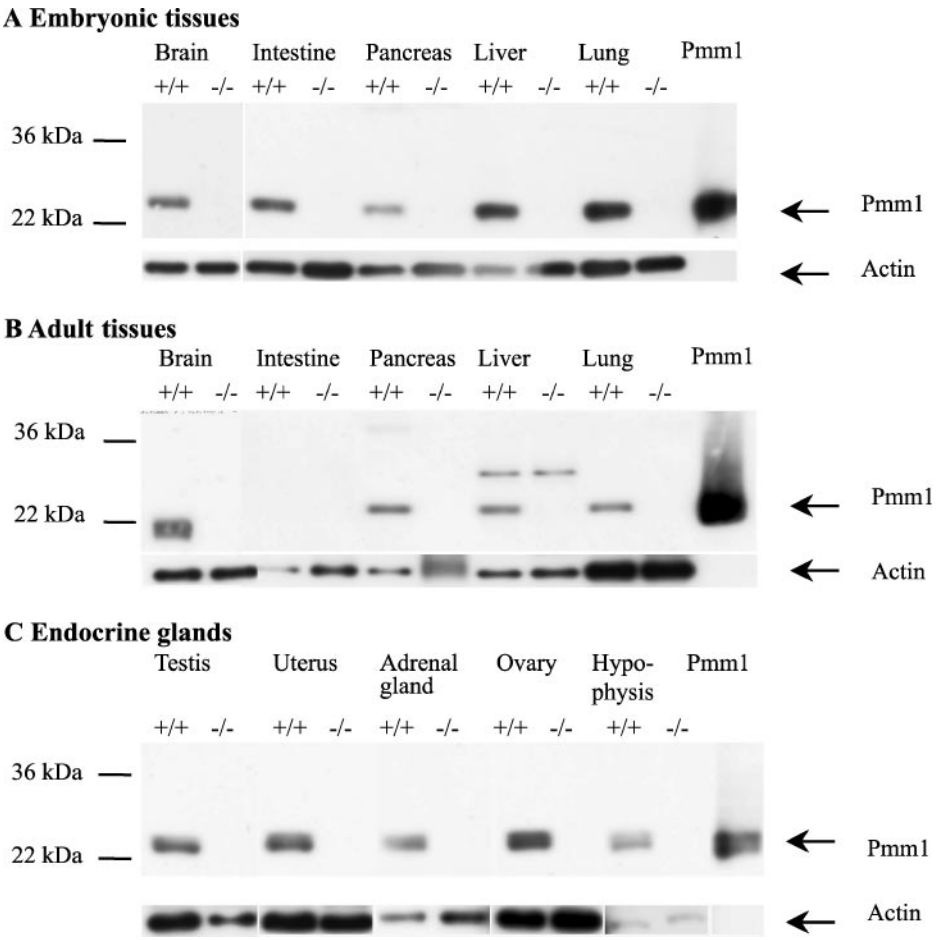

FIG. 2. Western blot analysis of embryonic (E17) (A) and adult (B) tissues and endocrine glands (C). Blots of tissue extracts (15 μg) and recombinant Pmm1 (10 ng) were probed with affinity-purified anti-Pmm1 antibody (1 in 10,000 for brain extracts; 1 in 500 for nonneural tissues) or with anti-β-actin antibody (1 in 5,000).The sizes of the molecular mass markers are indicated in kilodaltons.

RESULTS

Expression pattern of Pmm1 in wild-type mice by Western blot analysis. In the literature, data on the expression profile of Pmm1 have been limited to Northern blot analysis on human, rat, and mouse tissues and to Western blot analysis on rat tissues—and this only in the adult stage.

We traced Pmm expression by Western blotting expression analysis in the mouse both prenatally and in adulthood.

The data showed that Pmm1 expression levels are high in most tissues at both stages (Fig. 2A and B). The high expression level of Pmm1 in mouse embryos was characteristic for at least several embryonic tissues. Brain was the organ with the highest expression level. The signals for liver and lung were somewhat higher than for intestine and pancreas. These high expression levels were, however, downregulated postnatally. In adult intestine the Pmm1 concentration was below detection limits, whereas in the liver, pancreas, and lung the signal was low (Fig. 2B).

Stainings of whole embryos with the Pmm1 antibody (see below) revealed high expression levels in developing endocrine glands. Therefore, the adult glands were also analyzed on Western blot. Gonads, uterus, adrenal glands, and pituitary displayed a moderate expression level of Pmm1 (Fig. 2C).

Immunohistochemistry. To further analyze the cell types expressing Pmm1, we investigated embryonic and adult tissues by immunohistochemistry. In all Pmm1-positive regions, the staining was distributed throughout the cell body, in line with their documented localization (12).

Pmm1 expression in the embryonic mouse tissues. Staining of the E17 embryo with the Pmm1 antibody revealed strong signals in most organ systems: nervous system, gastrointestinal tract, endocrine glands, urinary system, and respiratory system. Epithelia such as the lung, gut, liver, and kidneys and endocrine glands such as the pancreatic islets, hypophysis, and adrenal gland were especially highly immunoreactive for Pmm1, as well as nervous system components, developing bone, muscle, and thymus.

(i) Nervous system. Nervous tissue components displaying high Pmm1 signals included peripheral ganglia, cerebellum, and cerebral cortex, including the hippocampus (Fig. 3A). Neurons in peripheral ganglia such as the spinal ganglia and the trigeminal ganglion were intensely labeled, as well as the peripheral, but not the central neurite branches of the sensory ganglia (Fig. 3B and C).

As described previously (7), Pmm1 signals in developing mouse brain were concentrated in cell bodies of neural stem

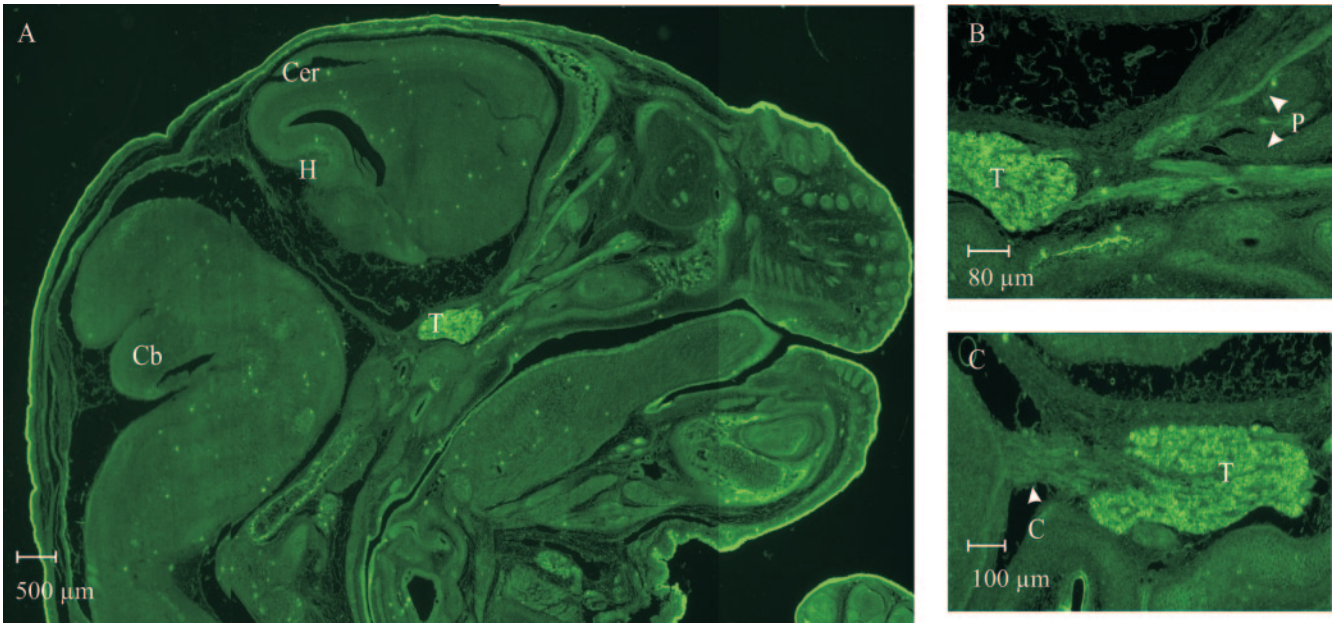

FIG. 3. Pmm1 immunoreactivity in the E17 head region. (A) Pmm1 signals have a widespread distribution throughout the developing brain, and particular intense signals are found in the sensory ganglia. (B) Peripheral processes from these ganglia are intensely labeled for Pmm1 in contrast to the central processes (panel C). Abbreviations: C, central branches; Cb, cerebellum; Cer, cerebrum; H, hippocampus; P, peripheral processes; T, trigeminal ganglion.

cells in the ventricular zone (VZ) and postmitotic neurons of the forming cortical plate of the developing cortex. In developing hippocampus the signals were most intense in cell bodies of the pyramidal cells of the Ammon's horn and their progenitors in the VZ. In the cerebellar primordium, intense signals were observed in the immature granule cells of the external granular layer and the germinal trigone.

In dendrites and axons the signals were less intense and the molecular zone always displayed a weak signal. Central white matter tracts were always negative (data not shown).

(ii) Gastrointestinal tract. In the E17 embryo, epithelial cells of the mucous membrane lining the gastrointestinal tract showed Pmm1-positive signals in the esophagus, stomach, and intestines. The submucosa and muscular compartment never displayed immunoreactivity for Pmm1. The body of the stomach showed intense signals in the glandular mucous membrane (Fig. 4A). The epithelial lining of the mucosa of the small intestine showed an equal distribution of the Pmm1 signal in villi and crypts (Fig. 4B).

In the liver, Pmm1 is expressed in hepatocytes (Fig. 4C). Secretory acinar cells of the exocrine pancreas were negative for Pmm1 (Fig. 4D).

(iii) Endocrine glands. The islets of Langerhans of the endocrine pancreas, visible as large clusters scattered throughout the secretory cells, showed intense Pmm1 immunoreactivity (Fig. 4D). In the developing adrenal gland isolated cell groups were highly Pmm1 immunoreactive (Fig. 4E).

(iv) Urinary system. Staining of the developing kidney with the Pmm1 antibody revealed high signals in the cortical region, whereas the medullary region was somewhat less stained. In the cortex, glomeruli were especially intensely labeled. Signals were less pronounced in the cortical proximal and distal convoluted tubules and in the components of the collecting system in the medullary region (Fig. 4E).

(v) Respiratory system. The lung alveoli, which at this stage are still collapsed, showed intense signals in the epithelial cells that do not yet have their mature squamous appearance as in expanded alveoli but are still cuboidal in shape. Terminal bronchi are less intensely stained (Fig. 4F).

Pmm1 expression in adult tissues. Tissues analyzed in detail included brain, intestine, pancreas, testis, ovary, and adrenal gland.

(i) Nervous system. The high Pmm1 immunoreactivity seen in the embryonic nervous system is maintained in the adult brain. Intensely labeled regions include the cortex, hippocampus, cerebellum, and olfactory bulb. As in the embryo, intense staining was almost completely restricted to neuronal cell bodies. Immunoreactivity with dendrites resulted in weak neuropil staining. Glial cells in the gray matter were mostly negative as were white matter tracts.

As described previously, Pmm1 signals in the adult brain were mostly restricted to neuronal cell bodies: the neurons of all cortical layers (Fig. 5A), Purkinje cells and, to a lesser extent, the cerebellar granular cells (Fig. 5B and C), granule cells in the adult dentate gyrus (Fig. 5D and E), pyramidal cells of CA1, CA2, and CA3, as well as some scattered polymorphic neurons.

Glial cells in gray and white matter tracts were mostly negative for Pmm1, as were axon tracts.

Intense staining in the olfactory bulb was observed in the mitral cell layer and the glomerular layer, whereas the signals were less intense in the granular layer and subependymal zone (Fig. 5F to H). The external plexiform layer was almost negative for Pmm1. In the glomerular layer staining was restricted

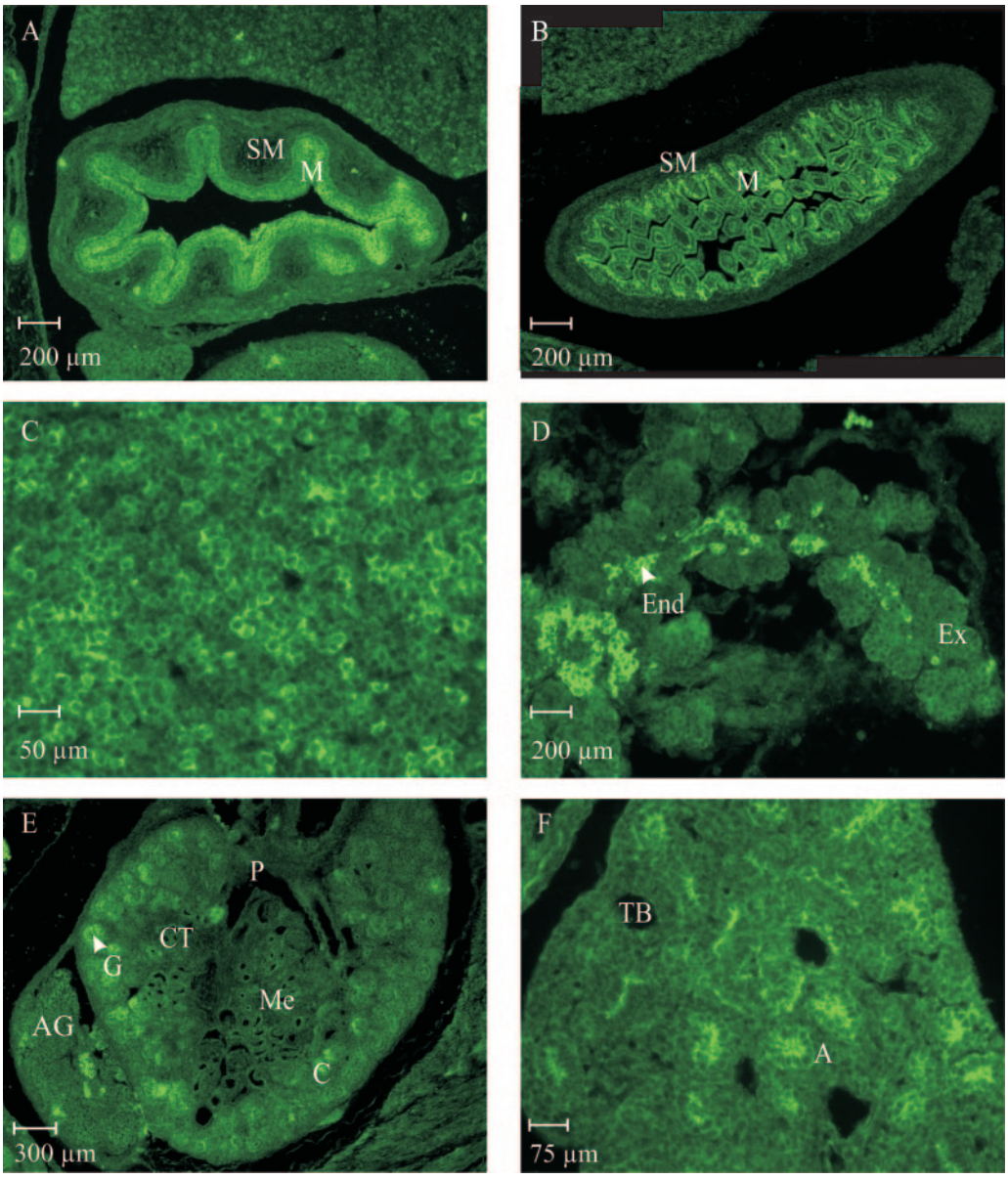

FIG. 4. Localization of the Pmm1 enzyme in developing visceral organs of the E17 mouse embryo. Intense staining in the mucosal lining of the stomach (A) and intestine (B). The surrounding submucosa is almost devoid of signal. (C) The liver parenchyma shows intense signals in hepatocytes. (D) Secretory cells of the exocrine pancreas are negative for Pmm1. The endocrine component is intensely stained with the anti-Pmm1 antibody. (E) In the adrenal gland the differentiating cells are Pmm1 positive, whereas in the developing kidney the glomeruli in the cortical region are highly immunoreactive. (F) The lung parenchyma is moderately stained, with intense signals in the epithelial cells lining the alveolar ducts. Abbreviations: A, alveolus; AG, adrenal gland; C, cortex; CT proximal or distal convoluted tubule; End, endocrine pancreas; Ex, exocrine pancreas; G, glomerulus; M, mucosa; Me, medulla; P, pelvic region; SM, submucosa; TB, terminal bronchus.

to the periglomerular cells, whereas the neuronal processes in the glomeruli were completely devoid of any signal (Fig. 5G). Also in the other layers, staining was restricted to the neuronal cells: mitral cells, granular cells, and a few scattered cells in the external plexiform layer (Fig. 5H).

(ii) Gastrointestinal tract. In the adult gut, Pmm1 expression was drastically downregulated. Whereas in the embryo the signals were equally distributed throughout the mucosa, in the adult gut the enterocytes of the villi showed remarkably low expression. Pmm1 signals were concentrated in the proliferative crypts (Fig. 6A), and occasionally signals were seen in goblet cells.

In the adult liver, Pmm1 signals were not distinguishable from the background signal (data not shown).

(iii) Endocrine glands. The adult adrenal gland revealed a region-specific expression with high Pmm1 signals in the cortex in contrast to the medullary region. In the cortex, the clusters of mineralocorticoid-secretoring cells of the zona glomerulosa showed particularly intense signals. The glucocorticoid-secreting cells in the other cortical layers, the zona fasciculata and

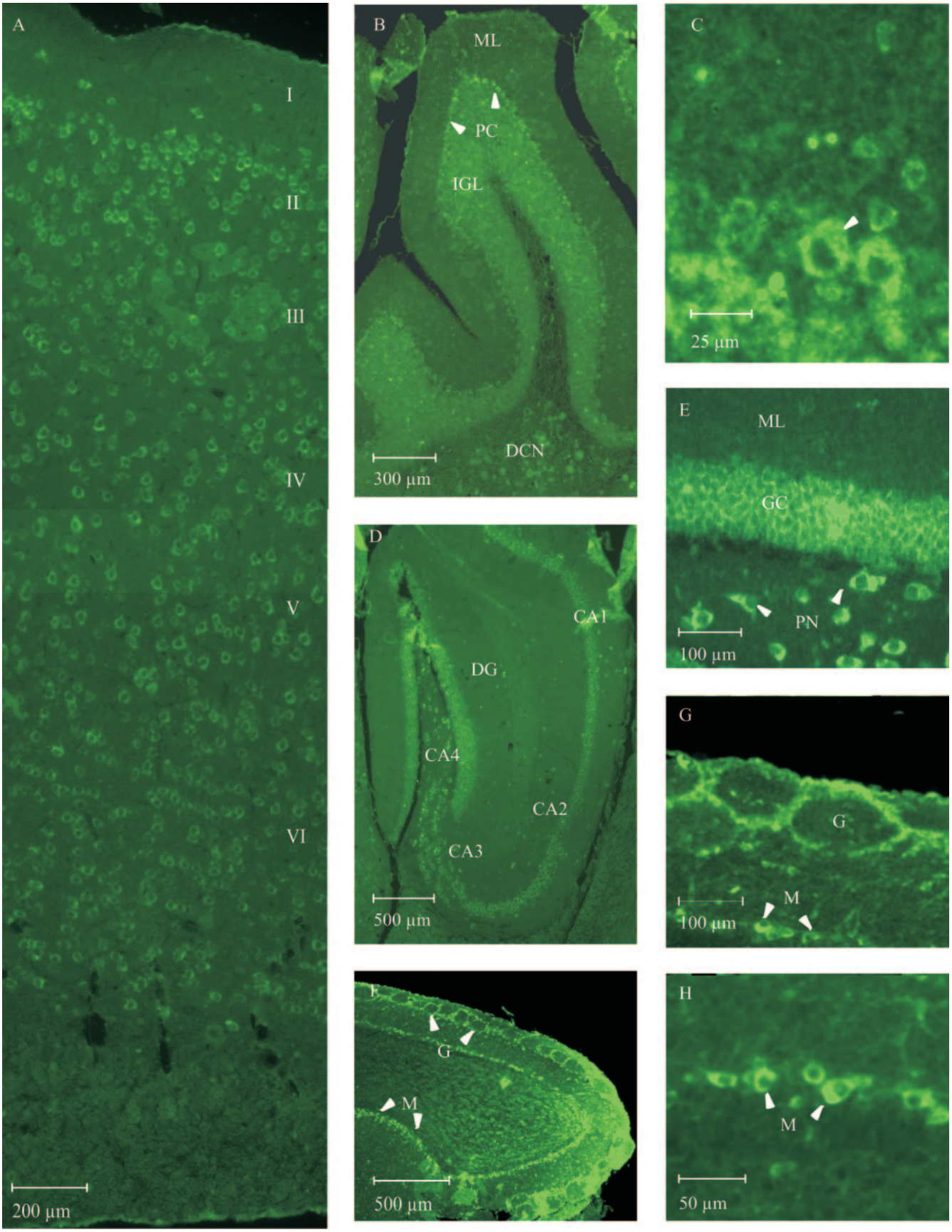
A
I
II
III
IV
V
VI
200 μm
B
ML
PC
IGL
DCN
300 μm
C
25 μm
D
CA1
DG
CA4
CA2
CA3
500 μm
E
ML
GC
PN
100 μm
F
G
M
500 μm
G
G
M
100 μm
H
M
50 μm

reticularis, displayed considerably weaker signals. Catecholamine-secreting cells of the medullary region were completely devoid of Pmm1 signals (Fig. 6B).

Immunohistochemical analysis of the gonads with the affinity-purified Pmm1 antibody revealed intense signals in distinct cell populations. A specific staining was observed in the spermatogonia of the seminiferous tubuli, whereas the more differentiated stages of the germ cells did not show Pmm1 signals. Sertoli cells and Leydig cells were negative (Fig. 6C). These results are, however, in contrast with the in situ analysis that showed a specific Pmm1 signal in the postmeiotic cells (Fig. 6D).

In the adult female gonads the ovarian germ cells displayed Pmm1 immunoreactivity: secondary follicles showed strong cytoplasmic staining, and weaker staining was observed in the zona granulosa and theca interna (Fig. 6E). The graafian follicles showed a particularly strong staining in the endocrine cells in the theca interna (Fig. 6F).

In the adult pancreas the Pmm1 signals are restricted to the islets of Langerhans (Fig. 7A and C). Double stainings for glucagon and insulin revealed Pmm1 is expressed in both cell populations (Fig. 7B and D).

Generation of Pmm1-deficient mice. Pmm1-deficient mice were generated by disruption of the coding region through insertion of a Neo cassette in exon 3 of the Pmm1 gene (Fig. 1A).

Southern blotting of eighty transfected ES cells revealed only one recombinant clone (Fig. 1B). After transfer of ES cells from this clone to pseudopregnant females, 19 pups were born. Eight of these pups were chimeric, and germ line transmission was observed with three male chimeras. Mutant mice homozygous for the Pmm1 gene disruption were obtained from heterozygote matings. Disruption of the Pmm1 gene was detected by allele specific PCR. The wild-type specific band of 330 bp was only apparent in the wild type and heterozygotes, whereas the 1.5-kb fragment was specific for the knockout allele (Fig. 1C). The disruption of the Pmm1 gene was confirmed by Southern blotting of genomic tail DNA, where the wild-type specific band of 11.5 kb is replaced by the targeted allele of 10 kb in Pmm1$^{-/-}$ mice (data not shown). The absence of Pmm1 protein in the Pmm1-deficient mice was shown by Western blotting of brain homogenates with the specific polyclonal anti-Pmm1 antibody (Fig. 1D).

Phenotypical analysis of Pmm1 knockout mice. Pmm1 knockout mice obtained on a mixed C57BL/6J background were backcrossed for five generations. The mice were viable and fertile and had normal litter sizes. They developed normally, without any major phenotype up to adulthood.

(i) Histological analysis. Analysis of the major Pmm1-expressing structures by light microscopy of hematoxylin-eosin sections did not reveal any pathologically alterations in the knockout mice (Fig. 8 and data not shown), although Pmm1 protein was clearly depleted, as demonstrated by immunohistochemistry of Pmm1 on sections of Pmm1-null mice (data not shown). Detailed histological screening of adjacent sections with markers of astroglial cells (antiglial fibrillary acid protein SMI-22 antibody) and microglia/macrophages marker (F4/80) did not reveal significant differences between wild-type and knockout mice (data not shown).

(ii) Behavioral assessment. The results of the behavioral tests are summarized in Table 2. Both the dusk-phase and overnight observations indicated comparable levels of cage activity for knockout and wild-type mice. In the open-field test, neither ambulatory measures (path length and corner entries), nor exploratory measures (entries and path length in center) differed significantly. Pmm1 knockouts and wild-type mice spent approximately equivalent amounts of time in the center or periphery of the open-field arena, as indicated by the center/periphery time ratios, an overall indicator of exploratory behavior and level of anxiety (Pmm1-null mice: 0.27; wild-type mice, 0.44). In the dark-light transition box, no significant differences in exploratory behavior were observed between the genotypes. Also, neither of the measures for social exploration were significantly different between knockout and wild-type mice.

Recordings of the walking pattern did not reveal any gait abnormalities or ataxia (data not shown), nor did the mice suffer from defects in motor learning, equilibrium, and coordination as manifested by normal performance on the accelerating rotarod test (i.e., a reportedly sensitive test for subtle deficits in cerebellar function). Despite abundant Pmm1 expression in Purkinje cells (7), Pmm1 knockout mice performed normal during four consecutive trials. Wire suspension also showed similar performance for knockout and wild-type mice.

Finally, learning and memory were evaluated with the passive avoidance test and Morris water maze. In passive avoidance learning, no differences in performance were observed between the groups. Spatial navigation learning was unaffected, as assessed in the Morris water maze test. No distinguishable differences were observed during eight acquisition trial blocks, and all animals learned to reach the escape plat-

FIG. 5. Localization of Pmm1 signals in adult mouse brain. (A) The expression of Pmm1 in the adult cerebral cortex was uniformly distributed over the six cortical layers, with the exception of layer I showing only faint neuropil staining. Ependymal and glial cells of the white matter were mostly negative. (B) In adult cerebellum, striking Pmm1-positive signals are seen in the Purkinje cell layer, whereas the granule cell layer has fainter signals, and the molecular layer is almost devoid of staining. Staining of the molecular layer was confined to faint neuropil staining. In the Purkinje cells (panel C, arrowhead) intense signals were observed in the cell body cytoplasm. (D) In the hippocampus, Pmm1 is expressed in adult CA regions and dentate gyrus. (E) Detailed photographs show high Pmm1 reactivity in dentate gyrus granular cell bodies and polymorphic neurons and faint neuropil staining in the molecular layer. (F) In the olfactory bulb intense signals are observed in the glomerular layer and the layer of mitral cells. (G) In the glomerular layer, the body of the glomeruli is devoid of Pmm1 signal, whereas surrounding nerve endings are intensely labeled. (H) In the mitral cell layer especially, the cell bodies of the mitral cells are immunoreactive for the Pmm1 antibody. Abbreviations: CA, cornus ammonis; DCN, deep cerebellar nuclei; DG, dentate gyrus; EGL, external granular layer; G, glomerulus; GC, granular cells; IGL, internal granular layer; M, mitral cell; ML, molecular layer; PC, Purkinje cell; PN, polymorphic neuron. (Panels A to E were reprinted from the *European Journal of Neuroscience*, Fig. 2C and Fig. 3C, E, I, and K [7], with the permission of the publisher.)

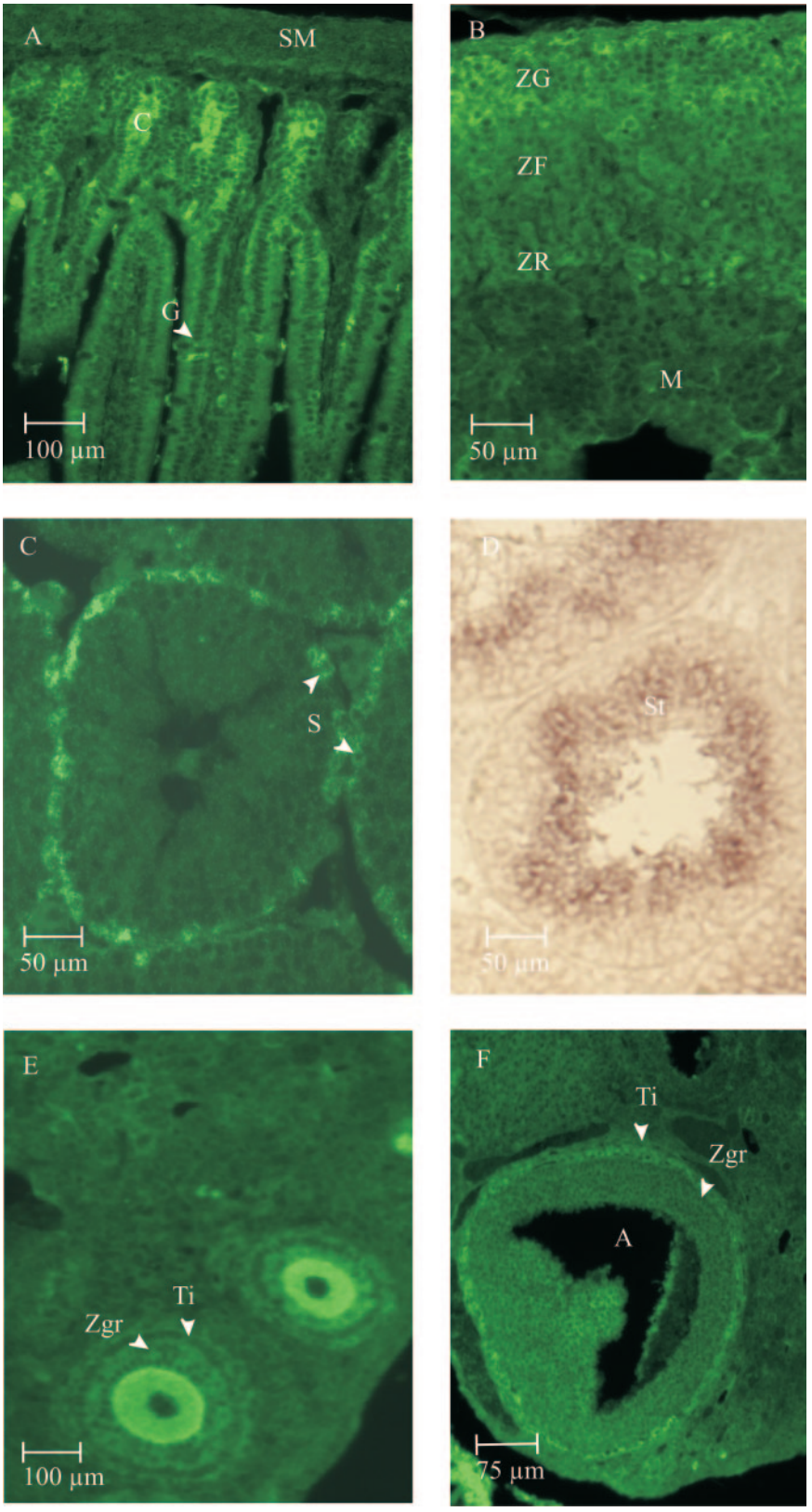

FIG. 6. Pmm1 immunoreactivity in adult mouse organs. (A) In the adult intestine Pmm1 signals are found in the mucosa, whereas the submucosa is almost devoid of Pmm1 signal. The Pmm1 signals are concentrated in the crypts, whereas in the villi Pmm1 the immunoreactivity is much less intense. (B) In the adrenal gland, especially the zona glomerulosa, cells show high immunoreactivity, whereas cells of the other layers are less intensely labeled. (C) In the seminiferous tubuli, spermatogonia are Pmm1 positive and not so much for the Sertoli and Leydig cells. (D) mRNA analysis reveals high signals in postmeiotic cells. (E and F) Strong cytoplasmic staining is seen in secondary follicles (E), and strong staining is obvious in the theca interna cells of the graafian follicles (F). Abbreviations: A, antrum; C, crypt; G, goblet cell; M, medulla; S, spermatogonium; SM, submucosa; St, spermatid; Ti, theca interna; ZF, zona fasciculate; ZG, zona glomerulosa; Zgr, zona granulosa; ZR, zona reticularis.

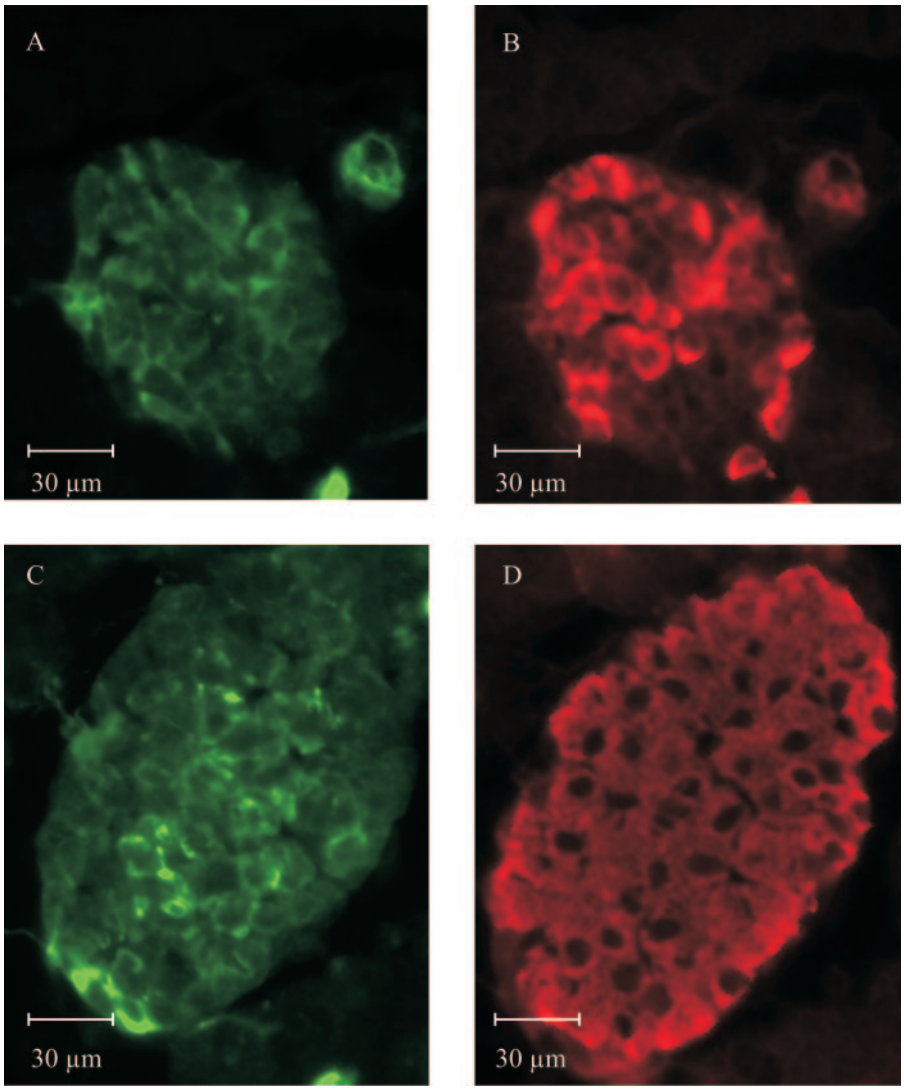

FIG. 7. Pmm1 localization in pancreatic cell populations. (A) Pmm1 shows a high expression level in pancreatic islets. (B) Staining of the same section with antiglucagon reveals a partial overlap in the signals. (C and D) Double stainings with an anti-insulin antibody also reveals a colocalization with pancreatic β cells.

form. During the probe trial, groups performed equally well and spent most time searching in the previously trained (target) quadrant (42% of the time for the knockout mice; 37% of the time for the wild-type mice).

In summary, Pmm1 knockout mice showed no abnormalities in general motor functions and performed similarly to their wild-type littermates in behavioral tests for learning abilities.

(iii) Glycohistochemical analysis. Although Pmm1 is highly expressed in brain throughout development, no differences in lectin binding patterns were observed between wild-type and knockout mouse brains in the stages investigated. None of the 21 lectins displayed an aberrant pattern in whole Pmm1 knockout embryos (details not shown).

(iv) Expression of Pmm2 in Pmm1-null mice. From previous studies it was clear that Pmm2 expression overlaps with Pmm1 in brain neurons (7). Because in vitro studies have shown Pmm2 is a functional homologue of Pmm1 (21), we tested whether Pmm2 was upregulated in Pmm1-deficient mice. The abundance of Pmm2 in homogenates from knockouts and wild-type littermates was assayed by Western blotting. The Pmm2 specific antibody showed similar levels in both Pmm1-knockout and wild-type mice (Fig. 9.).

DISCUSSION

PMM1 has the in vitro activity of a phosphomannomutase, but it is still uncertain whether this reflects its in vivo function. The fact that PMM1 does not seem to compensate a reduced phosphomannomutase activity due to deficiency of its homolog PMM2 either suggests a different physiological role or a different tissue expression. To understand the biological role of PMM1, we documented the expression of the murine protein in wild-type mice and generated Pmm1-deficient mice by knocking out the Pmm1 gene.

Our results first indicate that Pmm1 is almost ubiquitously expressed in the E17 embryo. In the adult mouse Pmm1 ex-

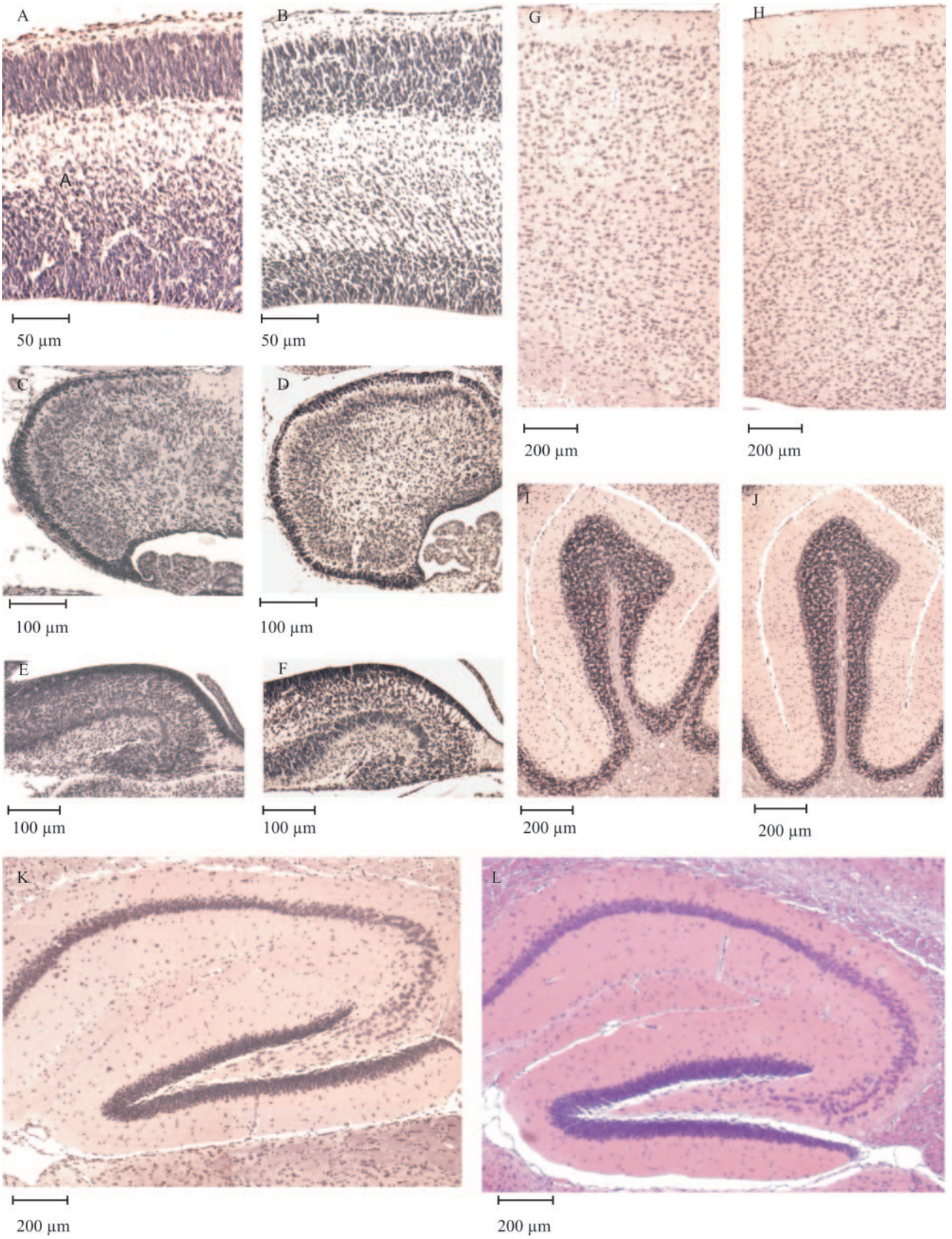

FIG. 8. Hematoxylin-and-eosin-stained sagittal sections of brain structures from wild-type and Pmm1 knockout embryonic (A to F) or adult mice (G to L). The results indicate that the Pmm1 deficiency does not affect cerebral cortex (A, B, G, and H), cerebellar (C, D, I, and J), or hippocampal development (E, F, K, and L).

TABLE 2. Summary of observations from behavioral studies performed with wild-type and Pmm1-knockout mice

Category	Mean ± SEM[a]	
	Wild-type mice	Pmm1 knockout mice
Cage activity (*n*)	17	15
Total beam crossings during the first 2 h	1,674 ± 711	1,605 ± 563
Total beam crossings during16 h	8,313 ± 3113	8,173 ± 3738
Open field (*n*)	7	6
Total path length (cm)	2,061 ± 858	2,745 ± 595
Corner entries	49 ± 17	61 ± 6
Entries in center	13 ± 10	27 ± 21
Path length in center (cm)	129 ± 111	289 ± 224
Dark-light transition (*n*)	17	15
Total beam crossings (first beam)	55 ± 24	58 ± 17
Total beam crossings (second beam)	41 ± 24	49 ± 20
Social exploration (*n*)	9	7
Total path length (cm)	2,064 ± 1316	2,154 ± 845
Entries in center	13 ± 8	14 ± 7
Path length in center (cm)	947 ± 813	890 ± 510
Rotarod (trial 4) (*n*)	17	15
Time on rod (s)	187 ± 89	211 ± 69
Wire suspension (*n*)	17	15
Latency of first slip (s)	47 ± 45	70 ± 47
Slips/120 s	3.6 ± 3.1	2.0 ± 2.2
Passive avoidance learning (*n*)	16	15
Step-through latency during training (s)	10 ± 3	12 ± 4
Step-through latency during testing (s)	261 ± 89	265 ± 85

[a] Data are means ± the standard errors of the mean except as noted. Statistical significance was determined by using the Student *t* test and analysis of variance.

pression changes to a more restricted pattern, with brain and endocrine glands displaying high signals. This argues for a function of Pmm1 both in embryonic development and in adult neuroendocrine tissues.

Surprisingly, knocking out the Pmm1 gene did not affect normal mouse development. Pmm1-deficient mice did not reveal any obvious abnormality and developed normally.

Pmm1 is ubiquitously expressed in the E17 embryo. We found high expression levels of the Pmm1 protein in the developing nervous system. Pmm1 is abundantly expressed in cells of proliferative zones such as the neuroblasts in the VZs and cerebellar germinal trigone. The epithelial layers of different organs such as the gastrointestinal tract and the respiratory and urinary systems of E17 embryos are highly immunoreactive as well. Moreover, the embryonic glands revealed considerable Pmm1 expression.

Pmm1 expression levels are downregulated in the adult mouse tissues. During adulthood, the high developmental Pmm1 expression was maintained in the brain, where Pmm1 signals were found in the neural cell bodies. In adult nonneural tissues the signals were downregulated, even below the detection level in the gut. Immunohistochemical analysis revealed Pmm1 mainly in the crypts, i.e., in or close to proliferating cells. Also, throughout the endocrine glands the high expression levels were maintained. This could argue for an important general function for Pmm1 in developing epithelial and neuronal tissues, whereas in the adult mouse Pmm1 is expressed in self-renewing stem cell populations such as the crypts of the adult intestine and cells with endocrine function.

Pmm1 expression and correlation with the CDG-Ia phenotype. Pmm1 is highly expressed in the tissues that are most severely affected in CDG-Ia, such as liver, kidney, gut, and brain (8, 29).

Of course, it is not clear yet whether the expression of Pmm1 in the CDG-Ia affected tissues corresponds to the localization of Pmm2 within these tissues. This will have to await the full documentation of the Pmm2 expression pattern.

In the brain, however, a complete expression pattern analysis was already presented for both Pmms (7). This revealed Pmm1 expression in the cerebellar granule and Purkinje cells. These cells are almost completely lost in CDG-Ia cerebellum (3, 5, 14, 15), probably due to a developmental defect progressing throughout early childhood (2, 10). The presence of Pmm1 in the external granular layer throughout cerebellar development is surprising, especially since Pmm2 is expressed in the exact same cell type and subcellular compartment (7).

The presence of Pmm1 in the most severely affected tissues in CDG-Ia and its exact colocalization with Pmm2 in the affected cell-types in the CDG-Ia brain confirm that Pmm1 cannot compensate for Pmm2 under in vivo conditions.

Pmm1-deficient mice are phenotypically normal. As judged by the expression data, loss of Pmm1 should have an impact on the developing brain and peripheral organs and possibly cell renewal in selected postneural tissues, i.e., follow an overall developmental motif of function. One could expect Pmm1-deficient mice to display deficiencies such as neurologic abnormalities, dysregulation of endocrine function, and fertility problems. However, we did not observe any of these abnormalities in our knockout animals. The Pmm1-deficient mice did not present a detectable phenotype and were indistinguishable from their wild-type littermates. They performed well on neurological tests, including tests for strength, balance, motor coordination, and learning. In addition, a detailed histological and glycohistochemical analysis did not reveal any abnormalities.

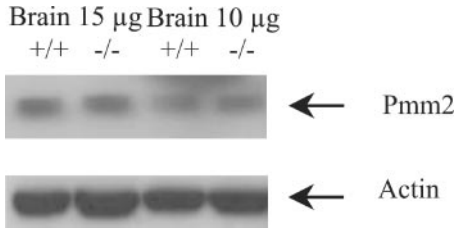

FIG. 9. Western blot analysis of Pmm2 in adult wild-type and knockout brain. Blots of brain extracts (10 and 15 μg) were probed with affinity-purified anti-Pmm2 antibody (1:10,000) or with anti-β-actin antibody (1:5,000), showing identical levels of Pmm2 in wild-type and knockout brain.

Lack of functional compensation by Pmm2. A possible explanation for the apparent normal condition of the Pmm1-deficient mice is redundancy, which is an evident outcome of gene duplication. In view of their similar in vitro activities, the most likely candidate as a compensating enzyme would be PMM2. However, a mutual compensation is unlikely since PMM1 cannot replace PMM2 in patients with congenital disorders of glycosylation (CDG) despite a broad overlap of their expression patterns (7). This suggests that the inability of Pmm1 to take over the Pmm2 function in brain is not due to a difference in expression pattern but more probably to a difference in physiological function. In line with this, Pmm2 expression levels were not upregulated in the Pmm1 knockout mice. Furthermore, our glycohistochemical and serum protein analysis in the Pmm1-deficient mice suggests that Pmm1 is not involved in protein glycosylation. To fully exclude this option, Pmm1 deficiency in a Pmm2-null background would have to be analyzed. Due to the early embryonic lethality of mice lacking Pmm2 (see accompanying study [25a]), this question cannot be directly answered and awaits the generation of mice with a partial loss of Pmm2 function surviving long enough for a meaningful analysis of an additional Pmm1 deficiency.

The genomic architecture of the human PMM and murine Pmm genes is remarkably well conserved, indicating that the original duplication event has occurred some 75 to 110 million years ago, well before mammalian radiation (25). Thus, the PMM genes would only be maintained in the genome for 100 million years if their duplication and divergence had a functional significance: without further selection one duplicate is inactivated with a half-life of 4 million years.

Indeed, compared to Pmm2, there are some regional differences in the expression pattern. In addition, Pmm1 encodes a phosphomannomutase that shows different substrate specificity and kinetics in in vitro assays (21). These observations argue for a different physiological role for PMM1 yet to be elucidated. From this standpoint, an alternative for the analysis of Pmm1 function might be subjecting the Pmm1-deficient mice to environmental challenge or the generation of mice overexpressing Pmm1.

Conclusion. Pmm1 is an enzyme that is widely but specifically expressed in embryonic and adult brain and endocrine glands. In most peripheral organs, high expression levels in the embryonic stage are downregulated at adulthood.

Despite the high expression levels in brain and endocrine glands, Pmm1 knockouts were viable and fertile and no histological abnormalities were observed in any of the major organ systems, including the nervous system and endocrine tissues that were studied in detail. Behavioral assays did not reveal any differences between Pmm1-null mice and wild-type mice. Glycan analysis of serum proteins and lectin glycohistochemistry did not reveal aberrant glycosylation patterns in the knockout.

The biological significance of Pmm1 may be revealed by crossing these mice with Pmm2-deficient mice or by challenging the Pmm1-null mice with different environmental factors.

ACKNOWLEDGMENTS

This study was supported by the Deutsche Forschungsgemeinschaft, the Fonds des Chemischen Industrie, the Koerber-Stiftung, the Fund for Scientific Research (FWO, Flanders 2, Belgium), the Interuniversity Poles of Attraction Federal Program, and the Fifth Framework Programme of the European Commission (EUROGLYCAN).

We thank Stephanie Grünewald and Natalie De Geest for help with antibody generation, testing of the antibodies, and histology.

REFERENCES

1. **Aebi, M., and T. Hennet.** 2001. Congenital disorders of glycosylation: genetic model systems lead the way. Trends Cell Biol. **11:**136–141.
2. **Akaboshi, S., K. Ohno, and K. Takeshita.** 1995. Neuroradiological findings in the carbohydrate-deficient glycoprotein syndrome. Neuroradiology **37:** 491–495.
3. **Antoun, H., N. Villeneuve, A. Gelot, S. Panisset, and C. Adamsbaum.** 1999. Cerebellar atrophy: an important feature of carbohydrate deficient glycoprotein syndrome type 1. Pediatr. Radiol. **29:**194–198.
4. **Artuch, R., I. Ferrer, J. Pineda, J. Moreno, C. Busquets, P. Briones, and M. A. Vilaseca.** 2003. Western blotting with diaminobenzidine detection for the diagnosis of congenital disorders of glycosylation. J. Neurosci. Methods **125:**167–171.
5. **Barone, R., L. Pavone, A. Fiumara, R. Bianchini, and J. Jaeken.** 1999. Developmental patterns and neuropsychological assessment in patients with carbohydrate-deficient glycoconjugate syndrome type IA (phosphomannomutase deficiency). Brain Dev. **21:**260–263.
6. **Crawley, J. N., J. K. Belknap, A. Collins, J. C. Crabbe, W. Frankel, N. Henderson, R. J. Hitzemann, S. C. Maxson, L. L. Miner, A. J. Silva, J. M. Wehner, A. Wynshaw-Boris, and R. Paylor.** 1997. Behavioral phenotypes of inbred mouse strains: implications and recommendations for molecular studies. Psychopharmacology **132:**107–124.
7. **Cromphout, K., L. Keldermans, A. Snellinx, J. F. Collet, S. Grunewald, N. De Geest, R. Sciot, E. Vanschaftingen, J. Jaeken, G. Matthijs, and D. Hartmann.** 2005. Tissue distribution of the murine phosphomannomutases Pmm1 and Pmm2 during brain development. Eur. J. Neurosci. **22:**991–996.
8. **de Lonlay, P., N. Seta, S. Barrot, B. Chabrol, V. Drouin, B. M. Gabriel, H. Journel, M. Kretz, J. Laurent, M. Le Merrer, A. Leroy, D. Pedespan, P. Sarda, N. Villeneuve, J. Schmitz, E. van Schaftingen, G. Matthijs, J. Jaeken, C. Korner, A. Munnich, J. M. Saudubray, and V. Cormier-Daire.** 2001. A broad spectrum of clinical presentations in congenital disorders of glycosylation I: a series of 26 cases. J. Med. Genet. **38:**14–19.
9. **Doucey, M. A., D. Hess, R. Cacan, and J. Hofsteenge.** 1998. Protein C mannosylation is enzyme-catalyzed and uses dolichyl-phosphate-mannose as a precursor. Mol. Biol. Cell **9:**291–300.
10. **Drouin-Garraud, V., M. Belgrand, S. Grunewald, N. Seta, J. N. Dacher, A. Henocq, G. Matthijs, V. Cormier-Daire, T. Frebourg, and P. Saugier-Veber.** 2001. Neurological presentation of a congenital disorder of glycosylation CDG-Ia: implications for diagnosis and genetic counseling. Am. J. Med. Genet. **101:**46–49.
11. **Grunewald, S., K. Huyben, J. G. de Jong, J. A. Smeitink, E. Rubio, G. H. Boers, H. S. Conradt, U. Wendel, and R. A. Wevers.** 1999. beta-Trace protein in human cerebrospinal fluid: a diagnostic marker for N glycosylation defects in brain. Biochim. Biophys. Acta **1455:**54–60.
12. **Hansen, S. H., S. R. Frank, and J. E. Casanova.** 1997. Cloning and characterization of human phosphomannomutase, a mammalian homologue of yeast SEC53. Glycobiology **7:**829–834.
13. **Heykants, L., E. Schollen, S. Grunewald, and G. Matthijs.** 2001. Identification and localization of two mouse phosphomannomutase genes, Pmm1 and Pmm2. Gene **270:**53–59.
14. **Horoupian, D.** 1995. Olivopontocerebellar atrophy in carbohydrate-deficient glycoprotein syndrome. Pediatr. Pathol. Lab. Med. **15:**175–179.
15. **Horslen, S. P., P. T. Clayton, B. N. Harding, N. A. Hall, G. Keir, and B. Winchester.** 1991. Olivopontocerebellar atrophy of neonatal onset and disialotransferrin developmental deficiency syndrome. Arch. Dis. Child **66:** 1027–1032.
16. **Jaeken, J., and H. Carchon.** 2001. Congenital disorders of glycosylation: the rapidly growing tip of the iceberg. Curr. Opin. Neurol. **14:**811–815.
17. **Jaeken, J., G. Matthijs, H. Carchon, and E. Van Schaftingen.** 2001. Defects of N-glycan synthesis, p. 1601–1622. *In* A. L. B. C. R. Scriver, W. S. Sly, and D. Valle (ed.), The metabolic and molecular bases of inherited diseases. McGraw-Hill Book Co., New York, N.Y.
18. **Matthijs, G., E. Schollen, C. Bjursell, A. Erlandson, H. Freeze, F. Imtiaz, S. Kjaergaard, T. Martinsson, M. Schwartz, N. Seta, S. Vuillaumier-Barrot, V. Westphal, and B. Winchester.** 2000. Mutations in PMM2 that cause congenital disorders of glycosylation, type Ia (CDG-Ia). Hum. Mutat. **16:**386–394.
19. **Matthijs, G., E. Schollen, E. Pardon, M. Veiga-Da-Cunha, J. Jaeken, J. J. Cassiman, and E. Van Schaftingen.** 1997. Mutations in PMM2, a phosphomannomutase gene on chromosome 16p13, in carbohydrate-deficient glycoprotein type I syndrome (Jaeken syndrome). Nat. Genet. **16:**88–92.
20. **Matthijs, G., E. Schollen, M. Pirard, M. L. Budarf, E. Van Schaftingen, and J. J. Cassiman.** 1997. PMM (PMM1), the human homologue of SEC53 or yeast phosphomannomutase, is localized on chromosome 22q13. Genomics **40:**41–47.
21. **Pirard, M., Y. Achouri, J. F. Collet, E. Schollen, G. Matthijs, and E. Van**

Schaftingen. 1999. Kinetic properties and tissular distribution of mammalian phosphomannomutase isozymes. Biochem. J. **339**(Pt. 1)**:**201–207.
22. **Pirard, M., J. F. Collet, G. Matthijs, and E. Van Schaftingen.** 1997. Comparison of PMM1 with the phosphomannomutases expressed in rat liver and in human cells. FEBS Lett. **411:**251–254.
23. **Pirard, M., G. Matthijs, L. Heykants, E. Schollen, S. Grunewald, J. Jaeken, and E. van Schaftingen.** 1999. Effect of mutations found in carbohydrate-deficient glycoprotein syndrome type IA on the activity of phosphomannomutase 2. FEBS Lett. **452:**319–322.
24. **Pohl, S., A. Hoffmann, A. Rudiger, M. Nimtz, J. Jaeken, and H. S. Conradt.** 1997. Hypoglycosylation of a brain glycoprotein (beta-trace protein) in CDG syndromes due to phosphomannomutase deficiency and *N*-acetylglucosaminyltransferase II deficiency. Glycobiology **7:**1077–1084.
25. **Schollen, E., E. Pardon, L. Heykants, J. Renard, N. A. Doggett, D. F. Callen, J. J. Cassiman, and G. Matthijs.** 1998. Comparative analysis of the phosphomannomutase genes PMM1, PMM2, and PMM2psi: the sequence variation in the processed pseudogene is a reflection of the mutations found in the functional gene. Hum. Mol. Genet. **7:**157–164.
25a. **Thiel, C., T. Lübke, G. Matthijs, K. von Figura, and C. Körner.** 2006. Targeted disruption of the mouse phosphomannomutase 2 gene causes early embryonic lethality. Mol. Cell. Biol. **26:**5615–5620.
26. **Wada, Y., A. Nishikawa, N. Okamoto, K. Inui, H. Tsukamoto, S. Okada, and N. Taniguchi.** 1992. Structure of serum transferrin in carbohydrate-deficient glycoprotein syndrome. Biochem. Biophys. Res. Commun. **189:**832–836.
27. **Wada, Y., and M. Sakamoto.** 1997. Isolation of the human phosphomannomutase gene (PMM1) and assignment to chromosome 22q13. Genomics **39:**416–417.
28. **Yamashita, K., H. Ideo, T. Ohkura, K. Fukushima, I. Yuasa, K. Ohno, and K. Takeshita.** 1993. Sugar chains of serum transferrin from patients with carbohydrate deficient glycoprotein syndrome: evidence of asparagine-N-linked oligosaccharide transfer deficiency. J. Biol. Chem. **268:**5783–5789.
29. **Zentilin Boyer, M., P. de Lonlay, N. Seta, M. Besnard, C. Pelatan, H. Ogier, J. P. Hugot, C. Faure, J. M. Saudubray, J. Navarro, and J. P. Cezard.** 2003. Failure to thrive and intestinal diseases in congenital disorders of glycosylation. Arch. Pediatr. **10:**590–595.